J Mater Sci (2007) 42:6171–6176
DOI 10.1007/s10853-006-1162-9

Creep behavior of AZ31 magnesium alloy in low temperature range between 423 K and 473 K

Ho-Kyung Kim · Woo-Jin Kim

Received: 30 March 2006 / Accepted: 18 October 2006 / Published online: 17 April 2007

Abstract The deformation behavior of coarse-grained AZ31 magnesium alloy was examined in creep at low temperatures below 0.5 T_m and low strain rates below 5×10^{-4} s^{-1}. The creep test was conducted in the temperature range between 423 and 473 K (0.46–0.51 T_m) under various constant stresses covering the strain rate range 5×10^{-8} s^{-1}–5×10^{-4} s^{-1}. All of the creep curves exhibited two types depending on stress level. At low stress ($\sigma/G < 4 \times 10^3$), the creep curve was typical of class I behavior. However, at high stresses ($\sigma/G > 4 \times 10^3$), the creep curve was typical of class II. At the low stress level, deformation could be well described by solute drag creep whereas at the high stress level, deformation could be well described by dislocation climb creep associated with pipe diffusion or lattice diffusion. The transition of deformation mechanism from solute drag creep to dislocation climb creep, on the other hand, could be explained in terms of solute-atmosphere-breakaway concept.

Introduction

Magnesium alloys are emerging as potentially good candidates for numerous applications, especially in the automotive industry due to their superior specific elastic modulus and specific strength, and so on [1]. Sufficient creep resistance is major requirement for use of magnesium alloys in automotive power-train components that are currently made in aluminum alloy or cast iron. Magnesium automatic transmission cases and engine blocks are used at elevated temperatures up to 473 K [2]. However, these alloys have poor creep resistance at temperatures above 400 K, which has made them inadequate for power-train applications. The poor creep strength of magnesium in these components can cause clamping load reduction in bolted joints, resulting in leakage in the power-train components.

Researches on creep deformation in pure magnesium and its alloys were mainly done at high temperatures ($T > 0.5$ T_m) [3–7]. For example, Vagarali and Langdon [4] performed creep tests on pure magnesium over the temperature 473–820 K. According to these authors, creep is controlled by dislocation climb. The activation energy for creep is independent of stress and is 135 kJ/mole, which is agreement with the value for lattice self-diffusion. The stress exponent is close to about 5 but increases to 6.5 at 473 K. Kim et al. [5] studied the deformation behavior of fine-grained AZ61 (Mg–6Al–1Zn) and AZ31 (Mg–3Al–1Zn) alloys in the temperature range 573–693 K and found that lattice diffusion controlled grain boundary sliding governs plastic flow at low strain rates and lattice diffusion controlled dislocation climb creep or pipe diffusion controlled dislocation climb creep governs plastic flow at high strain rates. Chung et al. [6] investigated the creep behavior of coarse-grained AZ31 alloy at 573–673 K. Viscous glide controlled creep, dislocation climb creep controlled by lattice diffusion and dislocation climb creep controlled by pipe diffusion showed up in order with increasing stress as the flow rate-controlling process.

H.-K. Kim
Department of Automotive Engineering, Seoul National University of Technology, 172 Kongnung-dong, Nowon-gu, Seoul 139-743, Korea

W.-J. Kim (✉)
Department of Materials Science and Engineering, Hongik University, 72-1 Sangsu-dong, Mapo-gu, Seoul 121-791, Korea
e-mail: kimwj@wow.hongik.ac.kr

Somekawa et al. [7] investigated creep behavior of coarse-grained Mg–Al–Zn alloys with different aluminum contents (3–9 Al%) covering the temperature range from 473 to 623 K. At high temperatures, the stress exponent was 5 and the activation energy was close to that for lattice diffusion of magnesium, whereas at low temperatures, the stress exponent was 7 and the activation energy was close to that for pipe diffusion for all alloys. They suggested that the climb-controlled dislocation creep was governed by pipe diffusion at low temperatures and by lattice diffusion at high temperatures in these alloys.

Though extensive studies have been conducted on creep behavior of magnesium alloys, their deformation behavior at low temperatures below 0.5 T_m, where the automotive power-train components operate, has rarely been reported [8–10]. Spigarelli et al. [8] investigated on AZ91 magnesium alloy in the temperature range from 393 to 453 K and described the minimum creep-rate dependence on applied stress by means of the sinh equation rather than the conventional power law due to that fact that the applied stresses used in the creep test were higher than the transition stress for power break-down.

The objective of this study was to evaluate creep resistance and investigate deformation mechanisms of coarse-grained AZ31 magnesium alloy in the low temperature range from 423 to 473 K (i.e., 0.46–0.51 T_m, T_m = 923 K based on T_m of pure magnesium) and in the low strain rate range from 5×10^{-9} s^{-1} to 5×10^{-4} s^{-1}. The present result was compared with Somekawa et al. [7] work on AZ31 alloy in the high strain rate range from 10^{-4} s^{-1} to 10^{-2} s^{-1} at 473 K.

Experimental procedures

All the creep tests were conducted using double-shear specimens from rods of conventionally extruded AZ31 magnesium alloy with a diameter of 25 mm. The nominal composition of the alloy is Mg–2.4Al–0.89Zn–0.39Mn in wt.%. The configuration and dimensions for the creep specimen is shown in Fig. 1. Prior to testing, all the specimens were annealed for 2 h at 693 K. The average grain size was found to be 98 μm after the heat treatment. The creep tests were conducted in air in a three-zone furnace. The test temperature was monitored with chromel–alumel thermocouples held in contact with the specimen and was maintained within ±1 K of the reported temperature. The strain during creep was measured with a linear variable differential transformer (LVDT), accurate to 1.7×10^{-3} mm. The LVDT signal was amplified, and monitored directly on a strip chart recorder. Details of the creep test procedure are described in the work by Kim et al. [11]. The shear stress, τ, and shear strain, γ, were converted to normal stress, σ, and normal strain, ε, using the expression $\sigma = 2\ \tau$ and $\varepsilon = 2/3\ \gamma$ [12]. The samples were tested at constant temperatures ranging from 423 to 473 K under various constant stresses.

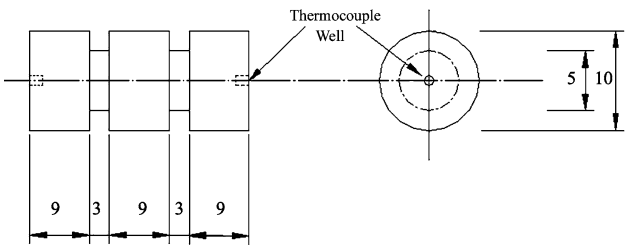

Fig. 1 Schematic of double-shear creep specimen geometry

Results and discussion

Creep curves

A large number of creep tests were conducted at stresses ranging from 10 to 140 MPa. All of the creep curves obtained in the present study exhibited two types depending on stress level. At low stresses, as shown in Fig. 2a, the shape of the creep curve was typical of class I (Alloy type) behavior [13]: there was a very small instantaneous strain on application of the load, and then a very brief primary stage which preceded steady-state flow. However, at high stresses, as shown in Fig. 2b, the shape of the creep curve was typical of class II (Metal type) behavior [13]: there is a normal primary creep stage, during which the creep rate decreases continuously with increasing time, that is then followed by a well-defined steady state period for which the creep rate remains essentially constant. The two types of creep curves are clearly illustrated by the plots shown in Fig. 3 of the logarithmic strain rate $\dot{\varepsilon}$ against the total strain ε for tests conducted at different stress levels at the same temperature. At the low stress (15 MPa), the primary stage is very brief. As the stress increases (40 and 120 MPa), the normal primary stage extends to higher strain.

Stress dependence of the steady state creep rate

The results from a number of tests conducted at three different temperatures under different stresses are shown in Fig. 4 in the form of steady state creep rate, $\dot{\varepsilon}$, against the applied tensile stress, σ, on a logarithmic scale. The data show that the value of stress exponent, n ($=\partial \ln \dot{\varepsilon}/\partial \ln \sigma$) was independent of temperature and that there is a significant variation in the stress exponent with stress level. The value of stress exponent was found to be 3.5 ± 0.2 at low stress level and 6 ± 0.5 at high stress level. The transition

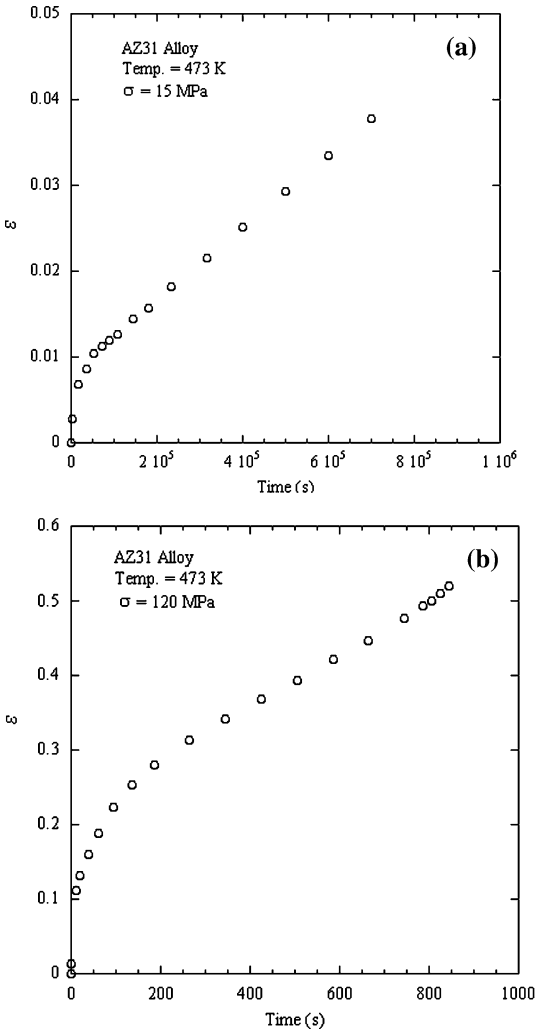

Fig. 2 Creep strain against time curves under (**a**) 15 MPa and (**b**) 120 MPa at 473 K

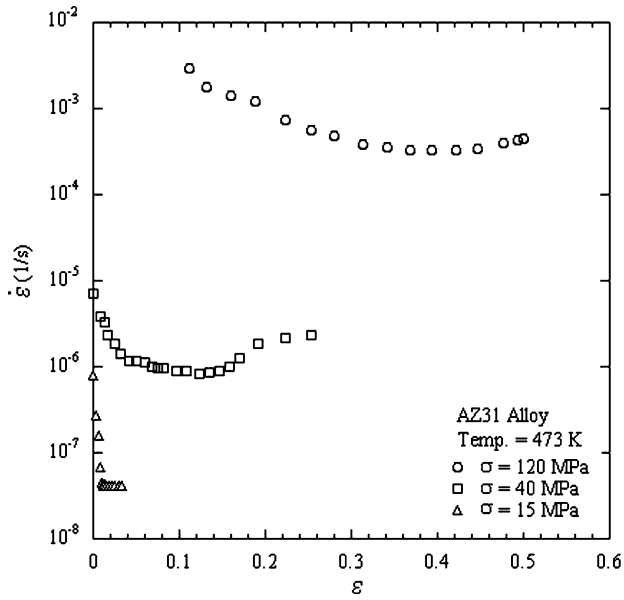

Fig. 3 Strain against strain for specimens tested at 473 K at different stress levels

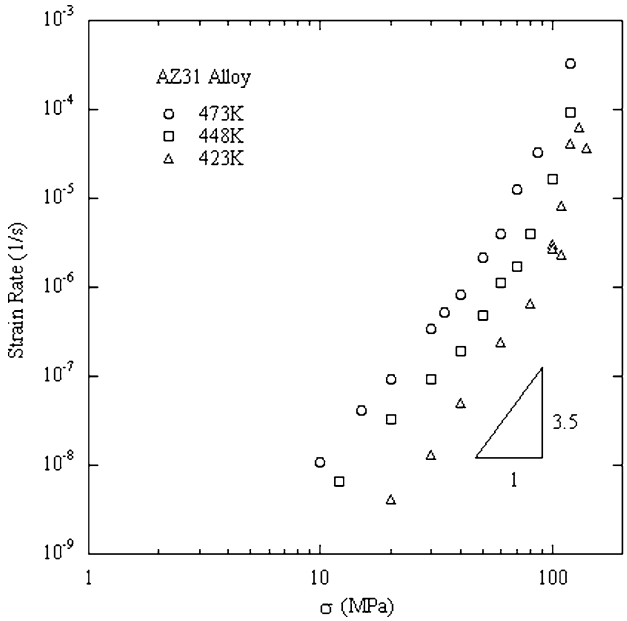

Fig. 4 Steady-state strain rate against stress in log–log format at temperatures between 423 and 473 K

stress delineating these two regions decreases with increasing temperature. A similar trend was reported in the coarse-grained AZ31 alloy where the value of n was 3 at low stress level and 6 at high stress level at the higher temperature range at 573–673 K [6].

Activation energy for creep

The constitutive equation for creep at elevated temperatures is generally depicted as an activation energy for creep can be determined using the power-law creep equation

$$\dot{\varepsilon} = AD_0 \exp\left(\frac{-Q}{RT}\right)\left(\frac{Gb}{kT}\right)\left(\frac{\sigma}{G}\right)^n \quad (1)$$

where $\dot{\varepsilon}$ is the steady state creep rate, n the stress exponent and A material constant, D_0 the pre-exponential factor for diffusion, G the shear modulus, Q the activation energy, R the gas constant and T the absolute temperature. For calculating the activation energy for the creep, the data of Fig. 4 were used to plot logarithmic $\dot{\varepsilon}G^{n-1}$ T against 1,000/T at low stresses (σ = 20, 30, 40 and 60 MPa) associated with n = 3.5 and at high stress (σ = 80 MPa) associated with n = 6. The result is shown in Fig. 5. The activation energy was then determined from the slope of the resultant

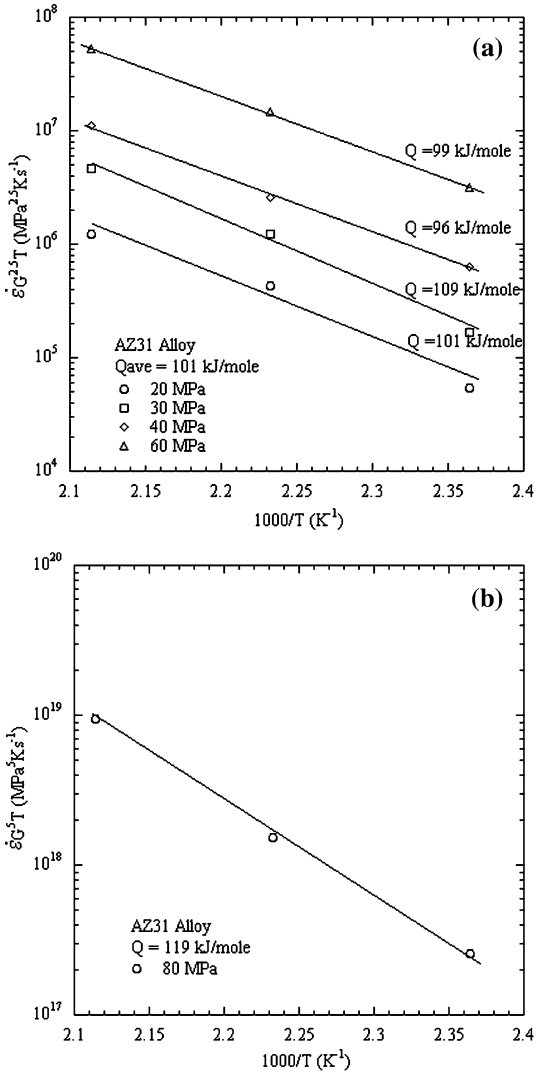

Fig. 5 Determination of the true activation energy for creep in AZ31 (**a**) at low stresses and (**b**) at high stress by plotting $\dot{\varepsilon}\, G^{2.5}T$ against $1/T$

straight line which, according to well-documented analysis [14], is equal to

$$-2.3R\left(\frac{d\log\dot{\varepsilon}}{d(1/T)}\right).$$

In estimating Q from the method, information concerning the shear modulus, G, was taken from the data available on the pure magnesium [15]. The modulus G for magnesium was expressed as 1.92×10^4–$8.6T$ (MPa). As noted in Fig. 5a, the average value of Q obtained from the analysis of the data is 101 kJ/mole at low stresses. As $n = 3$ is typically associated with solute drag creep, this value may be interpreted as that for the activation energy for Al diffusion in Mg (i.e., 143 kJ/mole [16]). The value of Q obtained at high stress (σ = 80 MPa) is, on the other hand, 110 kJ/mole. As $n = 6$ is typically associated with dislocation climb creep, this value can be interpreted as that for activation energy for lattice self-diffusion in magnesium (i.e., 135 kJ/mole [17]) or pipe diffusion in magnesium (i.e., 92 kJ/mole [15]). Thus, it can be expected that there is a transition to a new mechanism at high stress level.

Creep mechanism in AZ31 magnesium alloy

The experimental results therefore divided into two distinct types of behavior as follows;

Stress regime with n = 3.5 behavior

The experimental results in the region where $n = 3.5$ provide strong evidence that creep of the AZ31 alloy occurs by a viscous glide process as in class I behavior. The various points of agreement with this mechanism include not only the stress exponent close to 3 but also the lack of a significant instantaneous strain upon loading and the very brief normal primary stage of creep. In class I type creep, dislocations are understood to glide in a viscous manner due to their interaction with solute atoms. Several different drag processes have been proposed [18–20]. Among these mechanisms, calculations show that the major force retarding the glide of dislocations often arises from the presence of impurity atmospheres. In the theory of Weertman [18], it is assumed that the motion of dislocations occurs as sequential glide and climb processes, and the slower of these two processes is the rate-controlling mechanism. In the solid solution alloys when glide is slower than climb, the steady-state creep rate is given by

$$\dot{\varepsilon} = \frac{0.35}{e^2 c}\left(\frac{kT}{Gb^3}\right)^2\left(\frac{\bar{D}Gb}{kT}\right)\left(\frac{\sigma}{G}\right)^3 \tag{2}$$

where e is the solute-solvent size factor, c the solute concentration, k Boltzmann's constant (=1.38×10^{-23} J/K), b Burgers, $\overline{D}$ the chemical interdiffusivity of the solute atoms. On the other hand, the theory of Takeuchi and Argon [19] is based on Cottrell–Jaswan interaction. By considering the rates of dislocation multiplication and annihilation, the steady-state creep rate due to dislocation glide is given by

$$\dot{\varepsilon} = \frac{0.125}{e^2 c}\left(\frac{kT}{Gb^3}\right)^2\left(\frac{\bar{D}Gb}{kT}\right)\left(\frac{\sigma}{G}\right)^3 \tag{3}$$

In the theory of Friedel [20], it is assumed that the diffusion of solute atoms is assisted by the line tension of the dislocations. The steady-state creep rate is given by

$$\dot{\varepsilon} = 0.18\left(\frac{\bar{D}Gb}{kT}\right)\left(\frac{\sigma}{G}\right)^3 \quad (4)$$

To inspect the prediction of these three dislocation glide models, the datum points shown in Fig. 4 were replotted in logarithmic form of $\overline{D}kT/Gb$ against σ/G, putting $e = -0.1373$ [21], $b = 3.21 \times 10^{-10}$ m, $G = 1.92 \times 10^4$–$8.6T$ (MPa) [15] and taking $\overline{D}$ as the chemical interdiffusivity of aluminum in magnesium; $\overline{D} = 1.2 \times 10^{-3}$ exp (–143,000/RT) $m^2\ s^{-1}$ [4]. The effect of solid solution of zinc and manganese, which are minor alloys addition to Mg–Al–Zn system alloys, are neglected for the sake of simplicity, the solute (=aluminum) concentration $c = 0.022$. The results is shown in Fig. 6, and all of experimental points now reasonably well lie on a single line of slope of about 3 at low stresses but with an increase in slope at $\sigma/G > 4 \times 10^3$. Figure 6 shows also the predicted creep rates for the theories of Weertman [18], Takeuchi and Argon [19], and Friedel [20], as given by Eqs. (2)–(4), respectively. Within the region where $n = 3$, the present results are in better agreement with the prediction of Weertman and Friedel models [18, 20].

Stress regime with n = 6 behavior

There is a sharp deviation from the behavior with $n = 3$ at high stress; the stress exponent in this region is 6 and activation energy is 110 kJ/mole. This value is between the activation energy for lattice self-diffusion in magnesium (i.e., 135 kJ/mole [17]) and that for pipe diffusion in magnesium (i.e., 92 kJ/mole [15]). To identify the creep deformation mechanism in this regime, the data from Somekawa et al. [7] on AZ31 at 473 K at high stresses (over 90 MPa) covering strain-rate range from 10^{-4} s^{-1} to 10^{-2} s^{-1} are plotted together with the present data at the same temperature in Fig. 7. A good overlap is observed onto a single curve at the high stress regime associated $n = 6$. Somekawa et al. [7] showed that by incorporating the effective diffusion coefficient for magnesium, involving dislocation pipe diffusion and lattice diffusion, the data in the temperature range from 473 to 623 K can be described by a single relation for dislocation climb creep.

There have been several experimental investigations of solid solution alloys to examine the deviation at high stress from viscous glide behavior with $n = 3$. For example, Vagarali and Langdon [4] showed that there was marked change in the creep behavior of Al–Mg alloys with increasing stress such that there was an increase in the stress exponent from 3 to 4.5 and this change was due to the breakaway of dislocations from their solute atmospheres. Also, it was demonstrated that for various solid solution alloys, the values of the experimental stresses marking the transitions from viscous glide to a breakaway condition were in very good agreement with the stresses predicted by breakaway relationship developed by Friedel [20]. Following Friedel, the breakaway stress is expressed as

$$\tau_b = A_b\left(\frac{W_m^2 c}{kTb^3}\right) \quad (5)$$

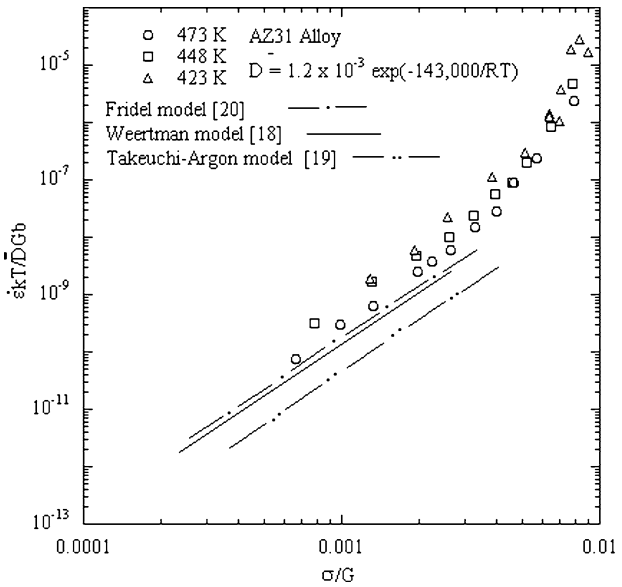

Fig. 6 Normalized strain rate against normalized stress for temperature from 423 to 473 K

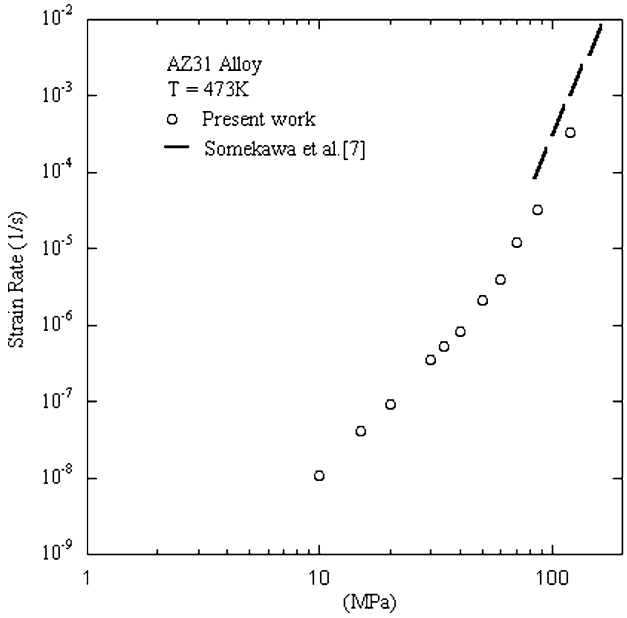

Fig. 7 Steady-state strain rate against stress in log–log format at 473 K

where τ_b is the shear stress necessary to break a dislocation from its solute atmosphere, A_b is a dimensionless constant, W_m is the maximum interaction energy between a solute atom and an edge dislocation and c is the solute concentration. The value of W_m is calculated from the theoretical expression [20]

$$W_m = -\frac{1}{2\pi}\left(\frac{1+v}{1-v}\right)G|\Delta V_a| \quad (6)$$

where ΔV_a is the difference in volume between the solute and solvent atom, v Poisson's ratio. For aluminum in magnesium, $\Delta V_a = 8.2 \times 10^{-30}$ m^3 [21]. The values of W_m at $T = 423$, 448 and 473 K were calculated, putting $b = 3.21 \times 10^{-10}$ m, $v = 0.34$, $G = 1.92 \times 10^4$–$8.6T$ (MPa) [15], $c = 0.022$ and $\sigma = 2\ \tau$. The value A_b is between 0.2 and 1 depending on model [22, 23]. If A_b is taken as 0.3, Eq. (5) can correctly predict the magnitude of the breakaway stresses of the present result. The predicted values of 63.0, 69.6 and 76.2 MPa for $T = 473$, 448 and 423 K, respectively, are very close to the experimental transition stress values of 60, 70, and 80 MPa for $T = 473$, 448 and 423 K, respectively.

Conclusions

The deformation behavior of coarse-grained AZ31 magnesium alloy was examined in creep at low temperatures below 0.5 T_m. The creep test was conducted in low temperature range from 423 to 473 K (0.46–0.51 T_m), under various constant stresses covering low strain rate range from 5×10^{-8} s^{-1} to 5×10^{-4} s^{-1}. The conclusions can be summarized as follows.

1. All of the creep curves exhibited two types dependent on stress levels. At low stress ($\sigma/G < 4 \times 10^3$), the creep curve was typical of class I behavior. However, at high stresses ($\sigma/G > 4 \times 10^3$), the creep curve was typical of class II.
2. At low stress level, deformation could be well described by solute drag creep whereas at high stress level, deformation could be well described by dislocation climb creep associated with pipe diffusion or lattice diffusion.
3. At low stress level where $n = 3.5$, the present results are in better agreement with the prediction of Weertman and Friedel models.
4. The transition of deformation mechanism from solute drag creep to dislocation climb creep could be explained in terms of solute-atmosphere-breakaway concept. This result indicates that the transition from solute drag creep to dislocation climb creep verified at high temperatures above 0.5 T_m is valid at low temperatures down to 423 K.

References

1. Friedrich H, Schumann S (2001) J Mater Process Technol 117:276
2. Luo AA (2004) Int Mater Rev 49:13
3. Vagarali SS, Langdon TG (1981) Acta Metall 29:1969
4. Vagarali SS, Langdon TG (1982) Acta Metall 30:1157
5. Kim WJ, Chung SW, Chung CS, Kum D (2001) Acta Mater 49:3337
6. Chung SW, Watanabe H, Kim WJ, Higashi K (2004) Mater Trans 45:1266
7. Somekawa H, Hirai K, Watanabe H, Tagigawa Y, Higashi K (2005) Mater Sci Eng A 407:53
8. Spigarelli S, Cabibbo M, Evangeliast E, Talianker M, Ezersky V (2000) Mater Sci Eng A 289:172
9. Shi L, Northwood DO (1994) Acta Metall 42:871
10. Evangerlista E, Spigarelli S, Cabibbo M, Scalabroni C, Lohne O, Ulseth P (2005) Mater Sci Eng A 410:62
11. Kim HK, Mohamed FA, Earthman JC (1991) J Test Eval 19:93
12. Isshiki K et al (1997) Metal Mater Trans 28A:2577
13. Cannon WR, Sherby OD (1970) Metall Trans 1:1030
14. Robinson SL, Sherby OD (1969) Acta Metall 17:109
15. Frost HJ, Ashby MF (1982) In: Deformation—Mechanisms Maps. Pergamon Press, Oxford, p 121
16. Moreau G, Cornet JA, Calais D (1977) J Nucl Mater 38:197
17. Shewmon PG, Rhines FN (1954) Trans Am Inst Min Engrs 200:1021
18. Weertman J (1957) J Appl Phys 28:1185
19. Takeuchi S, Argon AS (1976) Acta Metall 24:883
20. Friedel J (1964) In: Dislocations. Pergamon Press, Oxford, p 54
21. King HW (1966) J Mater Sci 1:79
22. Endo T, Shimada T, Langdon TG (1984) Acta Metall 32:1991
23. Kuchařová K, Saxl I, Cadek J (1974) Acta Metall 22:465